THE ACOUSTIC WAVEFIELD GENERATED BY A VESSEL SAILING ON TOP OF A STREAMER SPREAD

S. Hegna[1]

[1] PGS

Summary

During the acquisition of a source-over-cable survey in the Barents Sea, part of one sail line was repeated without triggering the airgun arrays. The acoustic signals associated with the vessel sailing on top of the streamer spread were recorded continuously by the streamers. This acquisition configuration offers an almost complete measurement of the wavefield generated by the vessel covering a large range of emission angles and frequencies. The acoustic wavefield generated by this vessel has been characterized from the measured direct arrivals. The image obtained after deconvolving this wavefield from the received wavefield will be presented and compared to the image obtained from an airgun source.

The acoustic wavefield generated by a vessel sailing on top of a streamer spread

Introduction

Estimating the acoustic wavefield generated by a seismic vessel when towing a streamer spread, and using this wavefield for imaging the subsurface, was presented in Hegna (2021). With such an acquisition configuration, only a limited part of the acoustic wavefield emitted from the vessel in the direction towards the streamers towed behind is measured directly and can be characterized. Also, because the streamers are towed far behind the vessel, the sea surface reflection, commonly referred to as the ghost, causes significant attenuation of the direct arrival. These factors limit the ability to characterize the acoustic wavefield generated by the seismic vessel, and the resulting seismic image did not contain information below 30 Hz because of this limitation. During the acquisition of a source-over-cable (Vinje et al., 2017) survey in the Barents Sea, part of one sail line was repeated without triggering the airgun arrays. The acoustic signals associated with the vessel sailing on top of the streamer spread were recorded continuously by the streamers. This acquisition configuration, illustrated in Figure 1, offers a much more complete measurement of the wavefield generated by the vessel covering a large range of emission angles and frequencies. The acoustic wavefield generated by this vessel was characterized from the measured direct arrivals. The image obtained after deconvolving this wavefield from the received wavefield will be presented and compared to the image obtained from an airgun source.

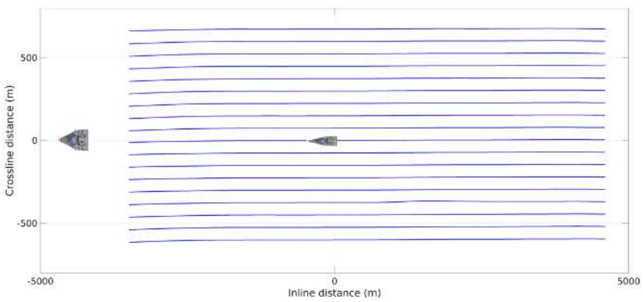

Figure 1 *Acquisition configuration with a vessel sailing on top of the multisensor streamer spread (blue lines). The seismic vessel in the front was towing 18 streamers with 75m separation. The streamer depth was 30m, and each streamer was 8km long.*

Method

Near-field hydrophones mounted close to individual source elements are commonly used for measuring the acoustic wavefield emitted by sources, and are standard equipment used in marine seismic data acquisition. Tests with a similar method, to investigate whether noise generated by propellers could be used as a seismic source, were discussed in Davies et al. (1992). The propeller signal was recorded with hydrophones protruded through the hull of a vessel just above the propeller. In Hegna (2021), the direct arrivals recorded by the streamers were used to characterize the wavefield generated by the seismic vessel towing the streamers. However, due to the acquisition configuration with a single vessel a long distance ahead of the streamers, only the signals emitted in the direction towards the streamers could be characterized. Furthermore, the seismic source was assumed to be omnidirectional. In this paper, the acoustic wavefield generated by a vessel sailing on top of the streamer spread, including its directivity, has been estimated from the recorded direct arrivals. This acquisition configuration offers a unique possibility to characterize the entire wavefield generated by the vessel. A grid of point sources has been used to represent the directional wavefield. The signals emitted from each of these grid points were determined using a similar approach as described in Hegna (2021). Firstly, the direct arrivals were isolated from the reflected signals. Secondly, the recorded direct arrivals were back propagated to the location of the grid points taking the directivity of the receiver arrays into account.

Examples

Figure 2 shows an example of raw recorded data recorded with 2ms temporal sample rate by the three streamers closest to the vessel sailing on top of the streamer spread. The strong amplitudes visible between channels 270 and 290 in each streamer are the direct arrivals from the vessel sailing above the streamers. These direct arrivals have been used to estimate the acoustic wavefield emitted by the vessel as described above.

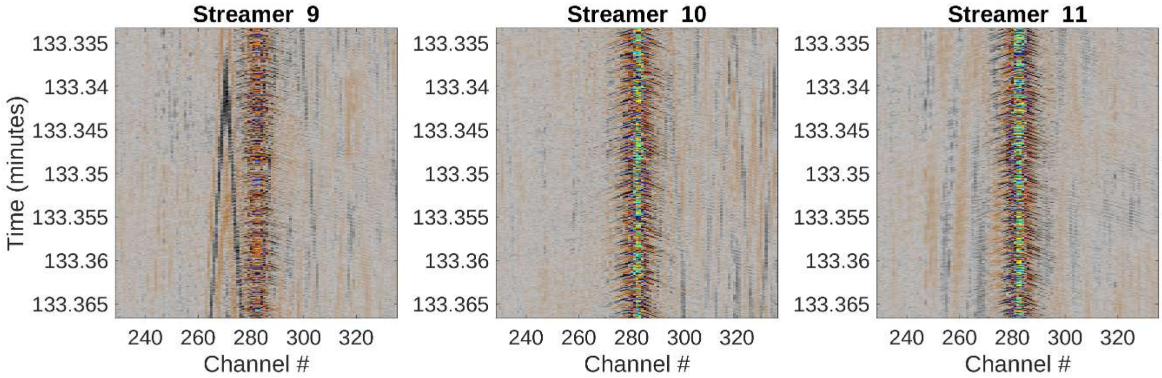

Figure 2 *Raw recorded hydrophone data recorded continuously by three streamers closest to the vessel sailing on top of the streamer spread.*

Figure 3 shows the amplitude spectrum of the pressure measurements recorded by the receiver group that is closest to the location of the vessel sailing above the streamers on average. The signals recorded by this channel are predominantly related to the direct arrivals. The amplitude spectrum shows that the acoustic signals generated by the vessel is very broadband. Distinct peaks at specific frequencies related to the rotational speed of the propellers and the number of blades on each propeller are clearly visible below ~100 Hz. Towards higher frequencies, the overall shape of the spectrum is very flat up to approximately 200 Hz where the anti-alias filter of the recording system starts to attenuate the signals. The broadband amplitude spectrum in combination with a random phase spectrum and continuous signals means that the acoustic wavefield generated by the vessel is approaching the properties of white noise.

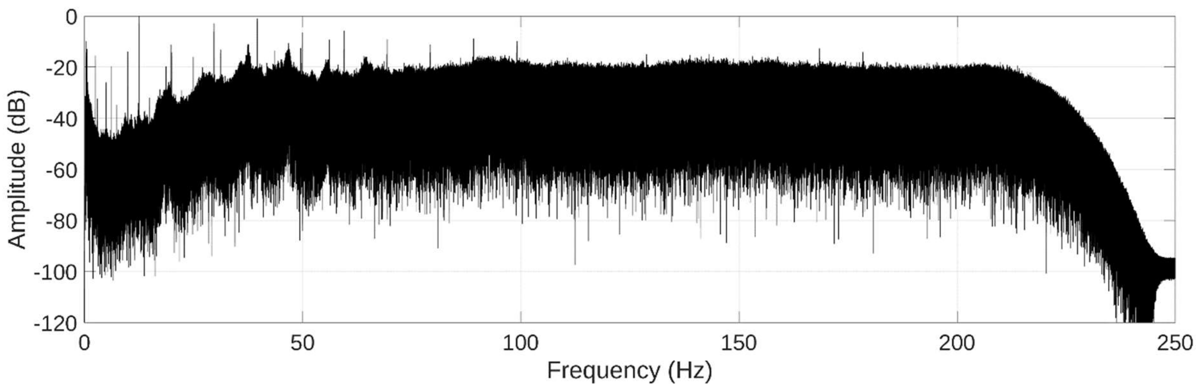

Figure 3 *Amplitude spectrum of raw recorded hydrophone data recorded by streamer 10, channel 281, that is on average closest to the vessel sailing on top of the streamer spread.*

The acoustic wavefield generated by the seismic vessel has been estimated from the recorded data using the method outlined above. Figure 4 illustrates the directivity of the estimated wavefield. Slightly more energy is emitted aft of the vessel in the inline direction. In the crossline direction the emitted signal levels appear to be slightly asymmetric with more energy emitted towards the port side of the vessel. But overall, the wavefield appears to be mostly omnidirectional without any deep notches in particular directions, and only minor variations with emission angle.

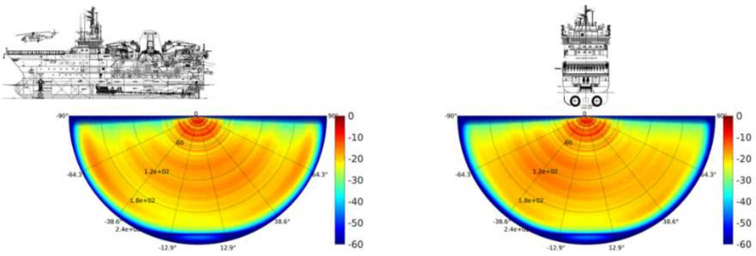

__Figure 4__ The inline (left) and crossline (right) directivity of the emitted acoustic wavefield from the vessel sailing on top of the streamer spread. The emission angles range from -90 to 90 degrees, and the displayed frequency range is from 0 to 240 Hz (the wavefield has been estimated up to 250 Hz).

The estimated wavefield emitted from the vessel sailing on top of the streamer spread has been used to predict and subtract the direct arrivals from the raw recorded pressure and motion sensor data, and the received wavefield has been separated into up- and down- going components. The estimated wavefield emitted from the vessel, i.e., the primary down-going wavefield, has then been deconvolved from the up-going pressure field in a multi-dimensional iterative fashion (Hegna et al., 2018) taking the motion of the source (the vessel) and the receivers into account. Since the test line was acquired along the same trajectory as parts of a line acquired by triggering airguns towed by the same vessel sailing on top of the streamer spread, the results obtained using the different sources can be compared. Figure 5 shows NMO stacks derived from data acquired without an active source and by triggering airgun arrays.

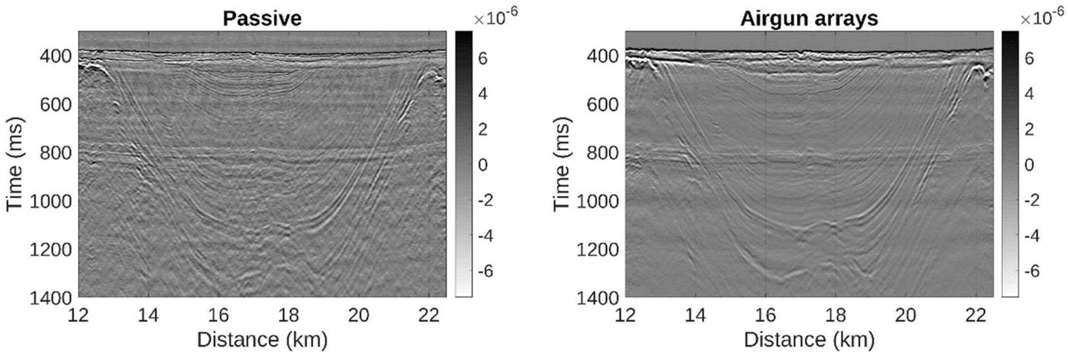

__Figure 5__ NMO stacks when using the signals emitted from the vessel sailing on top of the multisensor streamer spread as the source to the left, and with airgun arrays as sources to the right.

The comparison shown in Figure 5 shows a basin with steep flanks against shallow salt structures towards either end of the displayed window. The results obtained when using the acoustic wavefield generated by the vessel as the source may appear noisier compared to the NMO stack of the data acquired with airguns. However, on closer inspection, many details can be observed that are not related to noise. Figure 6 illustrates the level of detail that can be observed in the shallow parts of the section from the data acquired without an active source. The continuous source wavefield rather than discrete shot points every 37.5m is likely a significant contributory factor to the improved shallow resolution.

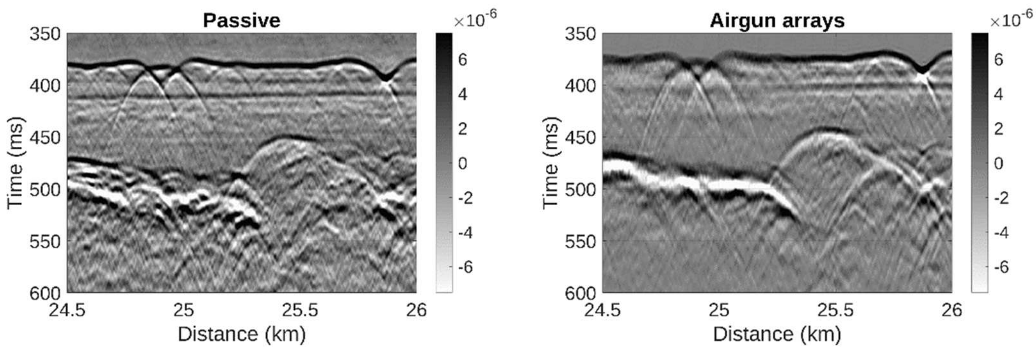

__Figure 6__ NMO stack from data acquired without an active source (left) and with airgun arrays (right).

Figure 7 shows octave panels from the NMO stack of the data acquired without triggering airgun arrays. There are coherent signals down to the 4-8 Hz panel in this NMO stack. The results presented in Hegna (2021) when using the signals emitted by the vessel towing the streamers showed no coherent signals below ~30 Hz. The reason why it is possible to resolve much lower frequencies with these data is the improved near offset coverage. The latter allows a more accurate estimation of the acoustic wavefield emitted from the vessel.

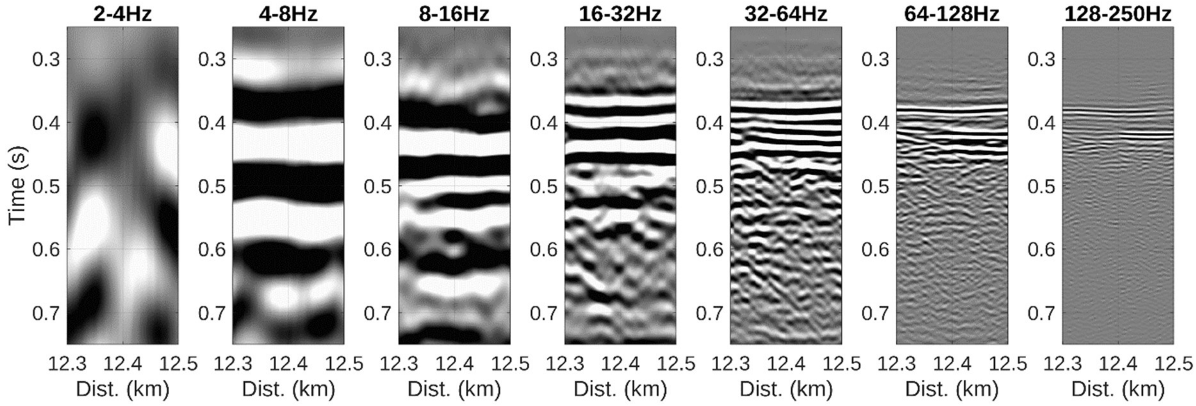

***Figure** 7 Octave panels from the NMO stack of the data acquired without active sources.*

Conclusions

The acoustic wavefield generated by a vessel sailing on top of a streamer spread can be determined from the recorded direct arrivals over a much larger range of emission angles and frequencies compared to the wavefield generated by a seismic vessel towing streamers far behind. The acoustic wavefield emitted by the vessel appears to be very broadband and almost omnidirectional with only minor variations related to emission angle.

An NMO stack of the conventional data acquired with airgun arrays has been compared to an NMO stack of the data acquired without triggering the airguns towed by the vessel sailing on top of the streamer spread. The results compare well. The results from the data acquired without active sources show many details at shallow depths, and exhibit very high temporal and spatial resolution. The bandwidth is very large, with coherent signals demonstrated from the 4-8 Hz octave band all the way up to 250 Hz.

Acknowledgements

I would like to thank Lundin Energy Norway AS and its partners DNO Norge AS and Petoro AS in PL1083 for permission to show the results from the Barents Sea test. Many thanks to PGS for supporting this work and for permission to publish the results.

References

Davies, K., Hampson, G., Jakubowicz, H. and Odegaard, J. [1992] Screw seismic sources. *62nd Annual International Meeting, SEG,* Expanded Abstracts, 710-711.

Hegna, S., Klüver, T., and Lima J. [2018] Making the transition from discrete shot records to continuous wavefields – Methodology. *80th Conference and Exhibition*, EAGE, Extended Abstracts, We LHR2 06.

Hegna, S. [2021] Continuous wavefields method – The acoustic wavefield generated by the seismic vessel. *82nd Conference and Exhibition*, EAGE, Extended Abstracts, 2021, 1-5.

Vinje, V., Lie, J.E., Danielsen, V., Dhelie, P.E., Siliqi, R., Nilsen, C.I., Hicks, E., and Camerer, A. [2017] Shooting over the seismic spread, *First Break*, **35**, 97-104.